Tension of toroidal magnetic field in reconnection plasmoids and relativistic jets

Krzysztof Nalewajko

Nicolaus Copernicus Astronomical Centre, Polish Academy of Sciences, Warsaw, Poland; knalew@camk.edu.pl

The toroidal magnetic field is a key ingredient of relativistic jets launched by certain accreting astrophysical black holes, and of plasmoids emerging from the tearing instability during magnetic reconnection, which is a candidate dissipation mechanism in jets. Tension of the toroidal field is an anisotropic force that can compress local energy and momentum densities. We investigate this effect in plasmoids produced during relativistic reconnection initiated from a Harris layer by means of kinetic particle-in-cell numerical simulations, varying the system size (including 3D cases), magnetisation, or guide field. We find that: (1) plasmoid cores are dominated by plasma energy density for guide fields up to $B_z \sim B_0$; (2) relaxed 'monster' plasmoids compress plasma energy density only modestly (by a factor of ~ 3 above the initial level for the drifting particle population); (3) energy density compressions by factors $\gtrsim 10$ are achieved during plasmoid mergers, especially with the emergence of secondary plasmoids. This kinetic-scale effect can be combined with a global focusing of the jet Poynting flux along the quasi-cylindrical bunched spine (a proposed jet layer adjacent to the cylindrical core) due to poloidal line bunching (a prolonged effect of tension in the jet toroidal field) to enhance the luminosity of rapid radiation flares from blazars. **(Nalewajko 2025, A&A, 696, A25; arXiv:2502.14954)**

Reconnection plasmoids: PIC simulations

We used a modified version of the public PIC code `Zeltron` (Cerutti et al. 2013, ApJ, 770, 147) to perform 2D and 3D simulations of relativistic magnetic reconnection in e^-e^+ pair plasma without radiation reaction in Cartesian coordinates with periodic boundaries. The resolution was $\mathrm{d}x = \rho_0/2.56$ with nominal gyroradius $\rho_0 = \Theta_e m_e c^2/eB_0$, relativistic temperature $\Theta_e = k_B T_e/m_e c^2 = 1$, nominal magnetic field strength $B_0 = 1$ G. We set two Harris layers (without perturbations) of thickness $\delta = 2\rho_0/u_{dr}$ determined by the drift velocity $\beta_{dr} = 0.3$; supported by the pressure of a drifting particle population of peak density $n_{dr,0} = \gamma_{dr} B_0^2/(8\pi\Theta_e m_e c^2)$; with background particle population of density n_{bg} to achieve magnetisation of $\sigma_0 = B_0^2/(4\pi n_{bg}\Theta_e m_e c^2)$. In some cases, we added guide field of strength B_g or third dimension with $L_z \gg \rho_0$. Simulations were performed for durations of at least $3L_x/c$. For example, simulation labeled L1800_σ10 was initiated with domain size $L_x = 1800\rho_0$ ($N_x = 4608$ cells) and $\sigma_0 = 10$.

Similar results were reported by Schoeffler et al. (2023, MNRAS, 523, 3812).

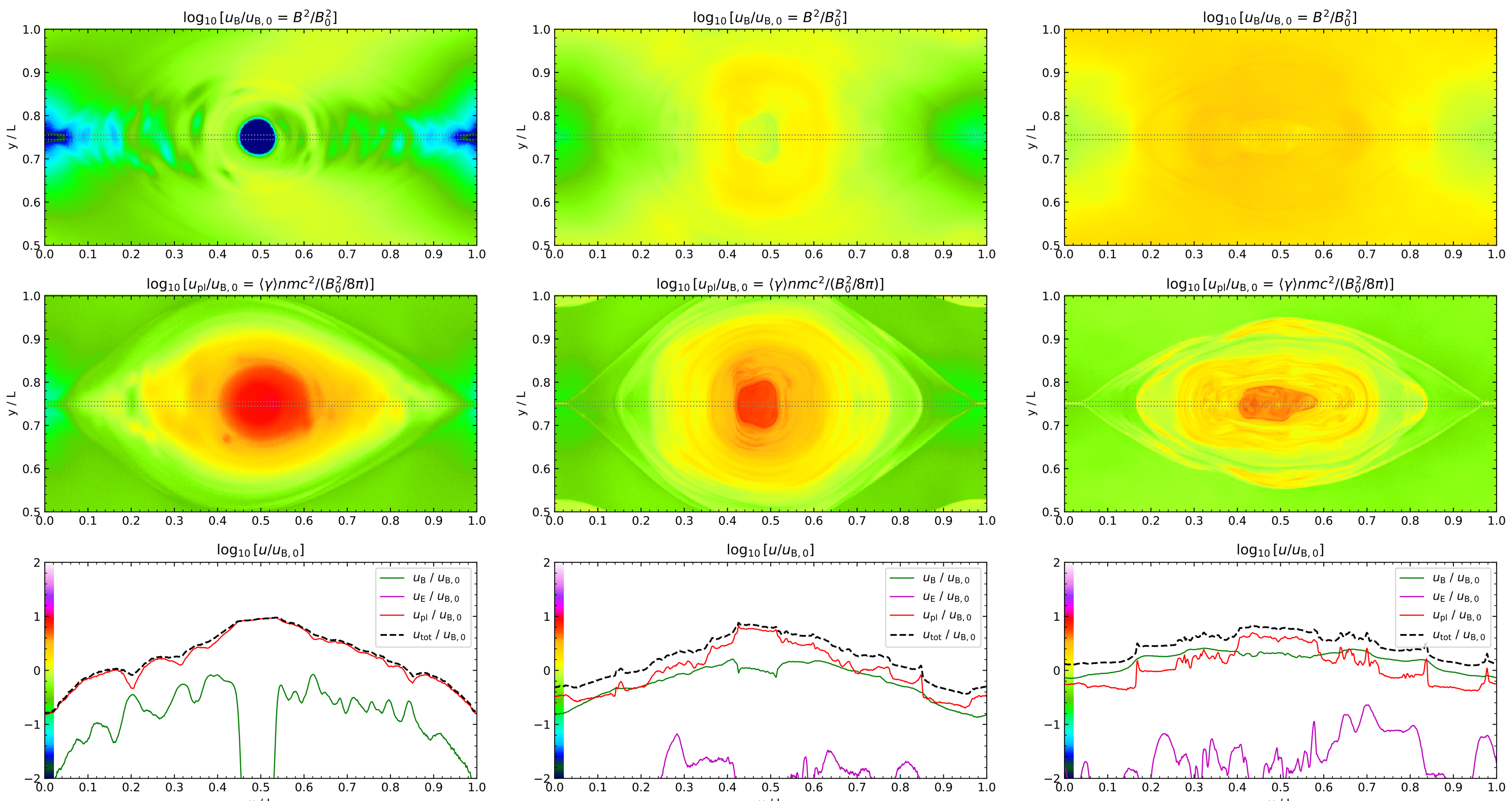

Figure 1: Maps of $\log_{10}(u/u_{B,0})(x,y)$ for magnetic energy density, $u_B = B^2/8\pi$ (upper panels), and plasma energy density, $u_{pl} = \langle\gamma\rangle nmc^2$ (middle panels), for relaxed monster plasmoids at the end of each simulation. In the lower panels, we compare 1D energy density profiles of $(u/u_{B,0})(x, y_0)$ measured along the strip indicated in the above maps by the dashed grey lines. A common colour scale for all maps is referenced along the left axes in the lower panels. Here, we present the effect of a guide field for $\sigma_0 = 10$ and $L/\rho_0 = 1800$. From the left, the columns show simulations: (1) L1800_σ10, (2) L1800_σ10_Bg05, and (3) L1800_σ10_Bg1.

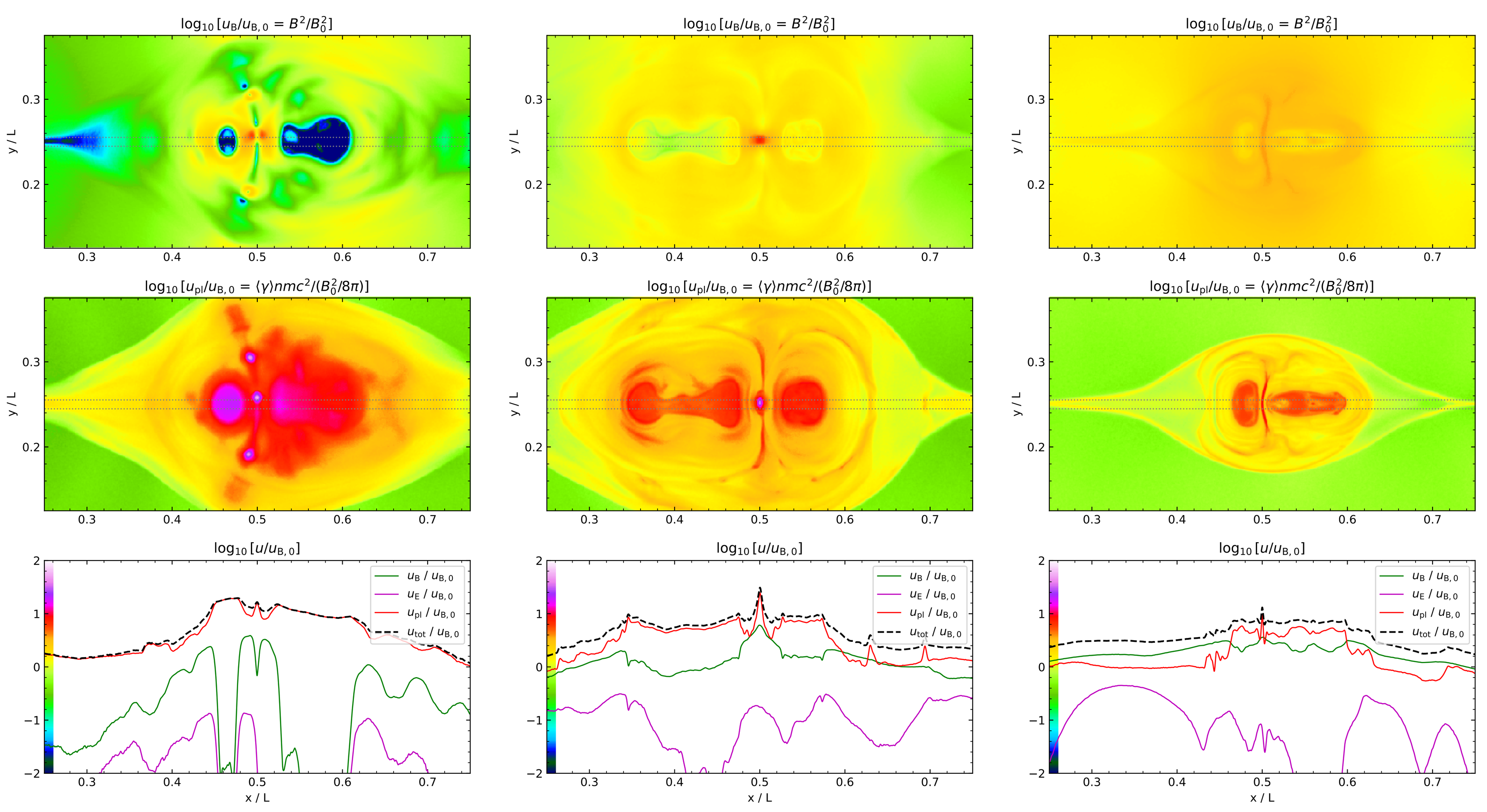

Figure 2: Same as Figure 1, but for plasmoid mergers that maximise the plasma energy density, u_{pl}, for the same set of simulations: (1) L1800_σ10, (2) L1800_σ10_Bg05, and (3) L1800_σ10_Bg1.

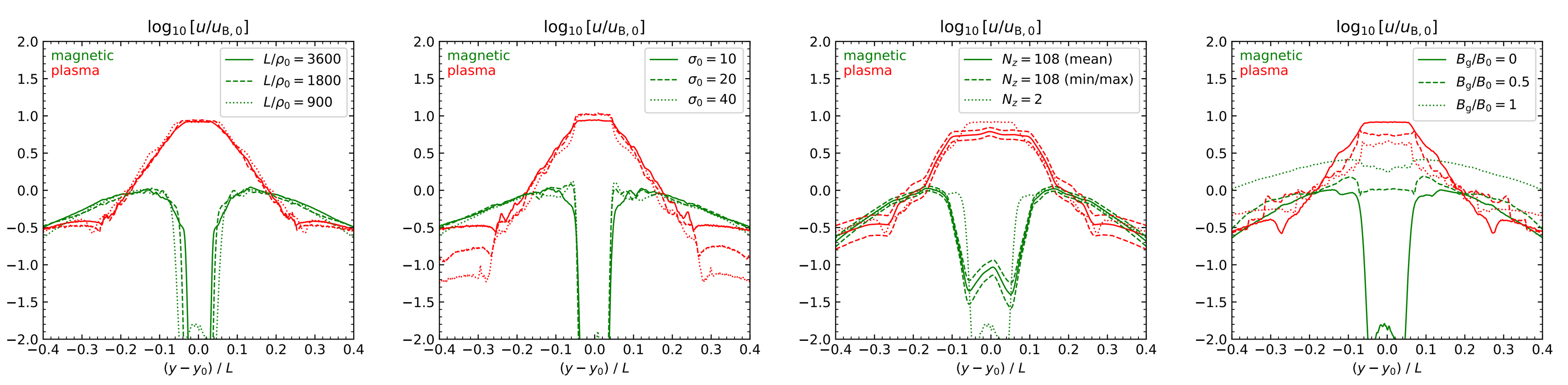

Figure 3: Profiles of magnetic (green lines) and plasma (red lines) energy densities across relaxed monster plasmoids. Panels from the left compare: (1) different sizes, L/ρ_0, of simulation domain (2D with $\sigma_0 = 10$, $B_z = 0$); (2) different magnetisations, σ_0 (2D with $L/\rho_0 = 1800$, $B_z = 0$); (3) 3D and 2D domains (with $L/\rho_0 = 900$, $\sigma_0 = 10$, $B_z = 0$); (4) different guide field strengths, B_g/B_0 (2D with $\sigma_0 = 10$, $L/\rho_0 = 1800$).

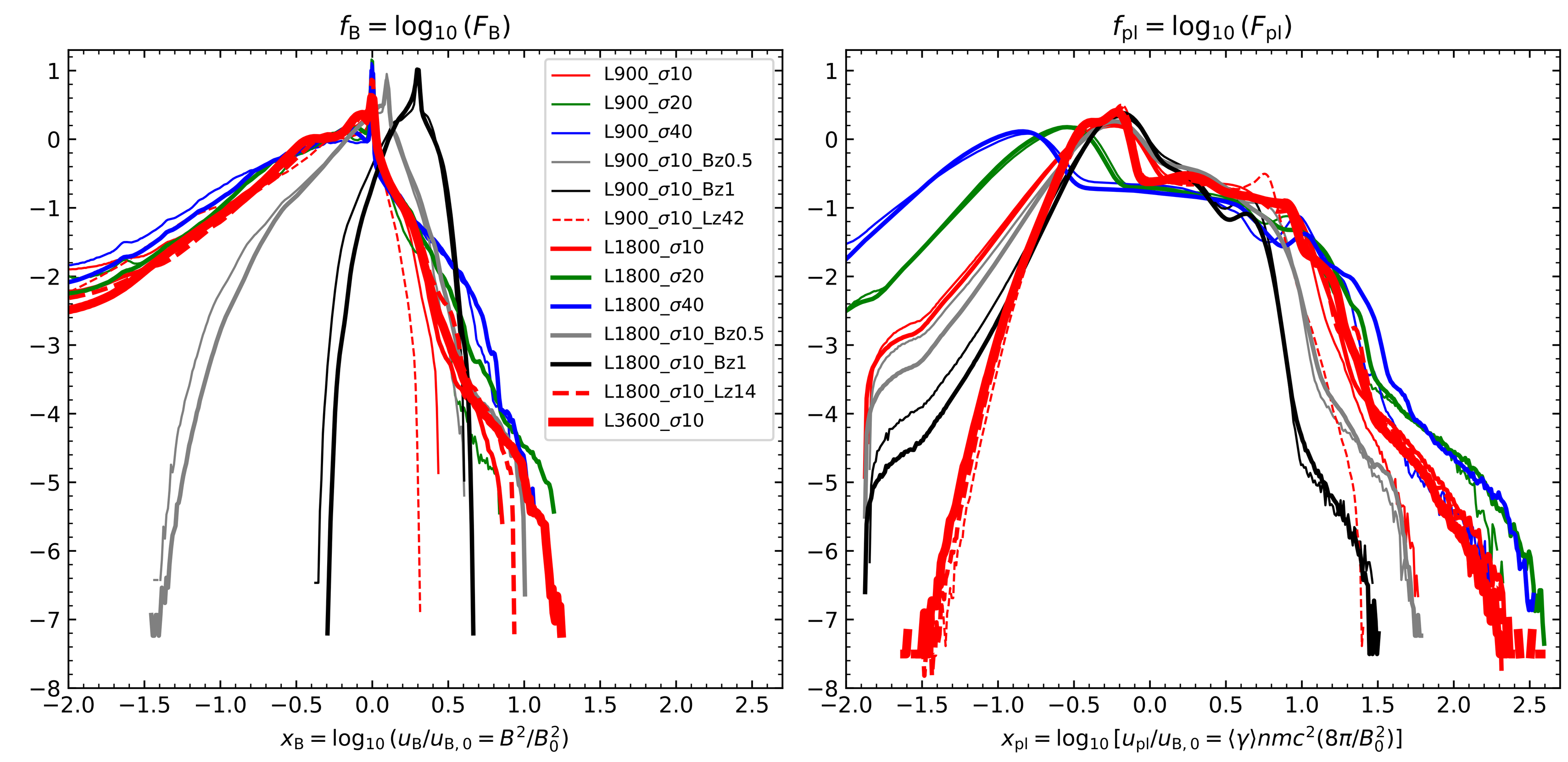

Figure 4: Logarithms, $f = \log_{10}(F)$, of volume distributions, $F(\mu) = \mathrm{d}F/\mathrm{d}\mu$, over the argument $\mu = \log_{10}(u/u_{B,0})$, with u the energy density: of magnetic fields, $u_B = B^2/8\pi$ (left panel), and of the plasma, $u_{pl} = \langle\gamma\rangle nmc^2$ (right panel). Functions $f(\mu)$ were averaged over the duration of each simulation.

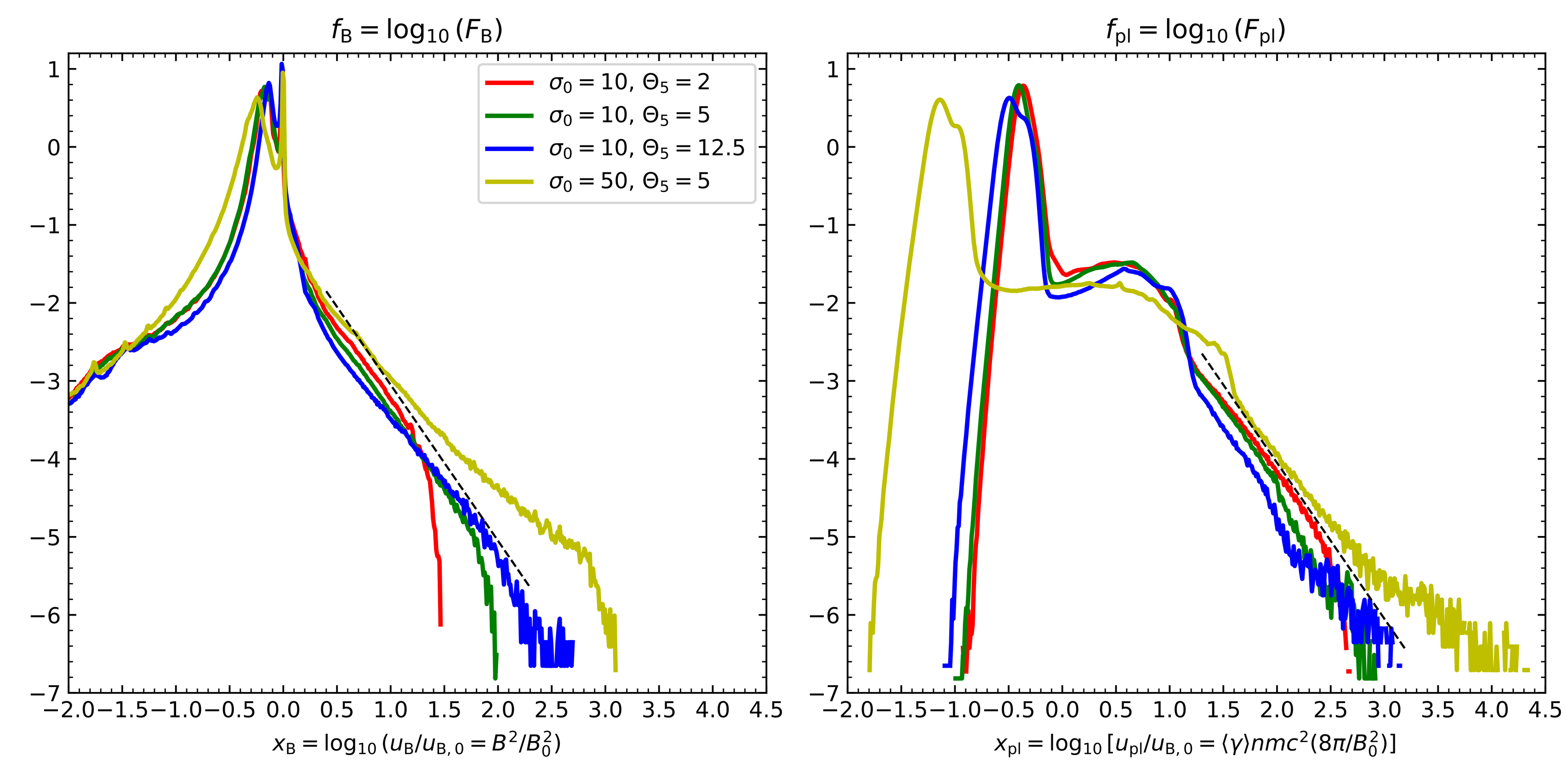

Figure 5: Same as Figure 4, but for the open-boundary simulations with synchrotron cooling presented in Ortuño-Macías & Nalewajko (2020, MNRAS, 497, 1365). Black dashed lines indicate power-law of index $-5/3$.

Relativistic jets: bunched spine

Consider the effect of toroidal field tension on the lateral structure of relativistic jet spine differentiated due to poloidal field bunching (Tchekhovskoy et al. 2009, ApJ, 699, 1789). Across the spine one can distinguish three zones: the innermost cylindrical *jet core*, the intermediate quasi-cylindrical *bunched spine*, and the outermost paraboloidal *main spine*. The main spine zone is the most extended and carries the bulk of the energy flux; it can be loaded by protons from the jet sheath via boundary instabilities (Chatterjee et al. 2019, MNRAS, 490, 2200), but this reduces the bulk Lorentz factor Γ. The bunched spine is the location of peak Γ, and peak toroidal magnetic field, B_ϕ, i.e., peak energy (Poynting) flux density. The jet core is prone to the current-driven instability (CDI), which can accelerate particles via high-σ reconnection (e.g., Ortuño-Macías et al. 2022, ApJ, 931, 137). CDI perturbations tend to spread from the most unstable toroidal field core to the outside. We propose that plasmoids from reconnection layers in the jet core spread to the bunched spine zone, where their enhanced energy density multiplies with the enhanced jet momentum flux density.

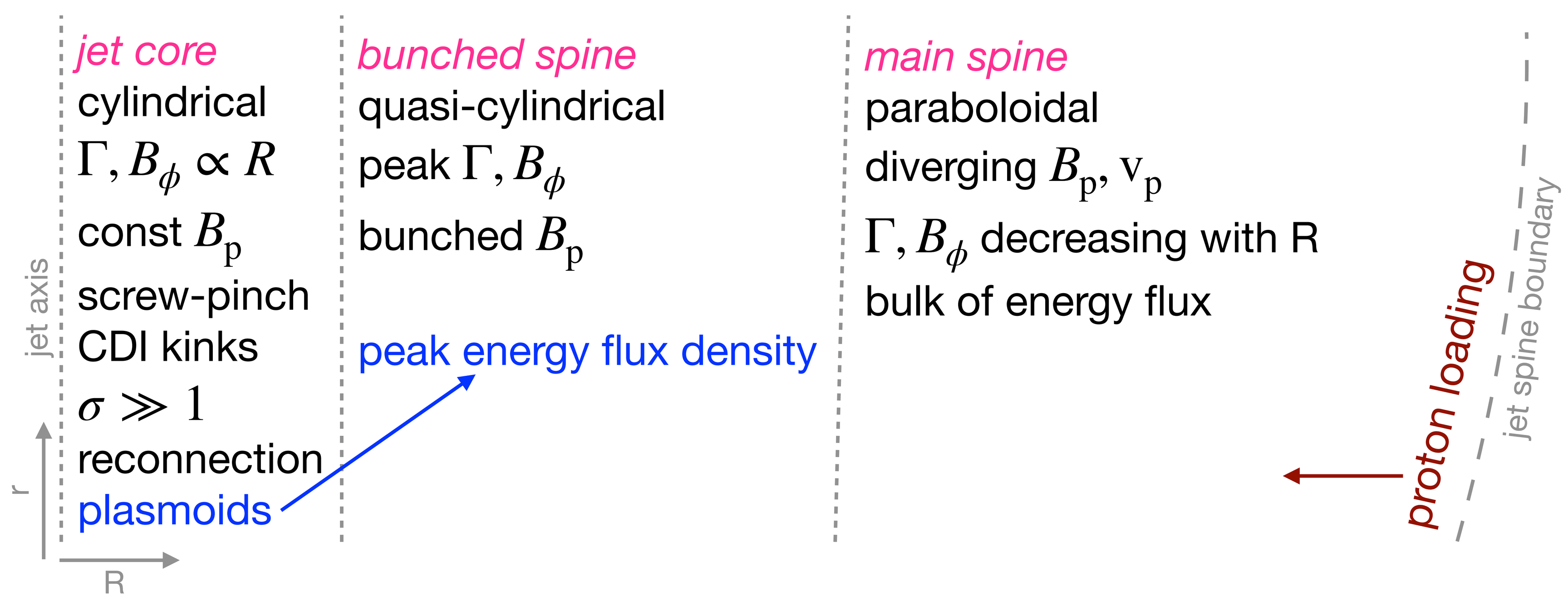

Figure 6: Proposed lateral structure (not to scale) of a relativistic jet differentiated due to poloidal field bunching. The *bunched spine* zone is introduced as the region maximizing the jet energy flux density. The introduction of plasmoids from reconnection layers created due to CDI in the jet core allow the energy density enhancement factors of the plasmoids and of the bunched jet spine to multiply.

This contribution was supported by the Polish National Science Centre grant 2021/41/B/ST9/04306.